JACS
JOURNAL OF THE AMERICAN CHEMICAL SOCIETY

Communication

pubs.acs.org/JACS

Alleviating Luminescence Concentration Quenching in Upconversion Nanoparticles through Organic Dye Sensitization

Wei Wei,[†] Guanying Chen,[†,‡] Alexander Baev,[†] Guang S. He,[†] Wei Shao,[†,‡] Jossana Damasco,[†] and Paras N. Prasad*[,†]

[†]Institute for Lasers, Photonics, Biophotonics, University at Buffalo, State University of New York, Buffalo, New York 14260, United States

[‡]School of Chemistry and Chemical Engineering, Harbin Institute of Technology, Harbin, Heilongjiang 150001, People's Republic of China

Supporting Information

ABSTRACT: The phenomenon of luminescence concentration quenching exists widely in lanthanide-based luminescent materials, setting a limit on the content of lanthanide emitter that can be used to hold the brightness. Here, we introduce a concept involving energy harvesting by a strong absorber and subsequent energy transfer to a lanthanide that largely alleviates concentration quenching. We apply this concept to Nd^{3+} emitters, and we show both experimentally and theoretically that the optimal doping concentration of Nd^{3+} in colloidal $NaYF_4$:Nd upconverting nanoparticles is increased from 2 to 20 mol% when an energy harvestor organic dye (indocyanine green, ICG) is anchored onto the nanoparticle surface, resulting in ~10 times upconversion brightness. Theoretical analysis indicated that a combination of efficient photon harvesting due to the large absorption cross section of ICG (~30 000 times higher than that of Nd^{3+}), non-radiative energy transfer (efficiency ~57%) from ICG to the surface bound Nd^{3+} ions, and energy migration among the Nd^{3+} ions was able to activate Nd^{3+} ions inside the nanoparticle at a rate comparable with that of the pronounced short-range quenching interaction at elevated Nd^{3+} concentrations. This resulted in the optimal concentration increase to produce significantly enhanced brightness. Theoretical modeling shows a good agreement with the experimental observation. This strategy can be utilized for a wide range of other lanthanide-doped nanomaterials being utilized for bioimaging and solar cell applications.

Lanthanide-doped upconversion nanoparticles (UCNPs) have great potential and a bright future in many areas, such as bioimaging, displays, solar cells, and biosensing.[1] These applications motivate scientific researchers to develop prescribed upconversion materials with bright upconversion luminescence (UCL). Yet, the low efficiency of upconversion nanomaterials is an immense concern for many practical applications. One of the most important reasons lies in the pronounced concentration quenching effect at high doping levels of the activator, which sets a limit on the amount of lanthanide emitters that can be used to produce luminescence. In most cases, the doping concentration of the activators is typically confined below 2 mol% to avoid the luminescence concentration quenching effect.[2] However, until now, limited progress has been made in solving this fundamental challenge. Jin's group reported that high-excitation irradiance can alleviate UCL concentration quenching in Tm^{3+}-doped UCNPs, as Tm^{3+} doping concentration increases from 0.5 to 8 mol%.[3] However, its realization has to rely on a suspended-core microstructured optical fiber in order to produce relatively high excitation irradiance (~10^6 W/cm^2), hindering numerous applications that require low excitation density such as *in vivo* bioimaging. In another report, Zhang's group was able to elevate the concentration quenching threshold of Er^{3+} from 2 to 5 mol% through a core/shell/shell/shell structure that spatially separates the emitter doping area through active domains incorporating high sensitizer Yb^{3+} concentration (20%).[2a] However, the core/shell/shell/shell structure is intricate and challenging to produce in terms of particle synthesis, and the approach is limited to UCNPs involving Yb^{3+} as the sensitizer, as it demands the first and the third shell to be doped with Yb^{3+} ions.

Herein, we introduce a simple and reliable approach to break the concentration quenching threshold and significantly boost the UCL of UCNPs through near-infrared (NIR) dye sensitization. We selected indocyanine green (ICG) as the NIR dye and colloidal upconverting $NaYF_4$:Nd as a model system. The ICG dye was selected because it possesses a large absorption cross section (~6×10^{-16} cm^2),[4] ~30 000 times higher than that of Nd^{3+} ions (~2×10^{-20} cm^2)[5] at 800 nm, and its emission band strongly overlaps with the absorption peaks of the Nd^{3+} ions, enabling efficient non-radiative energy transfer from ICG to surface Nd^{3+} ions (Scheme 1). The nanoparticles doped with Nd^{3+} alone are utilized because of the involved simple upconverting mechanism. We show that the optimal doping concentration of Nd^{3+} was shifted from 2 to 20 mol%, along with a 10-fold UCL enhancement through ICG dye sensitization (Scheme 1).

A series of $NaYF_4$:Nd UCNPs with increasing Nd^{3+} content were fabricated utilizing a method adapted from the literature.[6] TEM images (Figure 1a) show that all nanoparticles are uniform, with an average size of 18.2 ± 1.1 nm (Figure S1). The XRD results (Figure S2) indicate that all samples are of

Received: September 9, 2016
Published: November 4, 2016

DOI: 10.1021/jacs.6b09474
J. Am. Chem. Soc. 2016, 138, 15130−15133

Scheme 1. A Brief Description of the Optimal Nd^{3+} Doping Concentration with and without ICG Sensitization, and the Realization of Enhanced UCL with the Presence of ICG, with the Absorption Spectrum of Nd^{3+} and the Absorption and Emission Spectra of ICG Shown in the Center

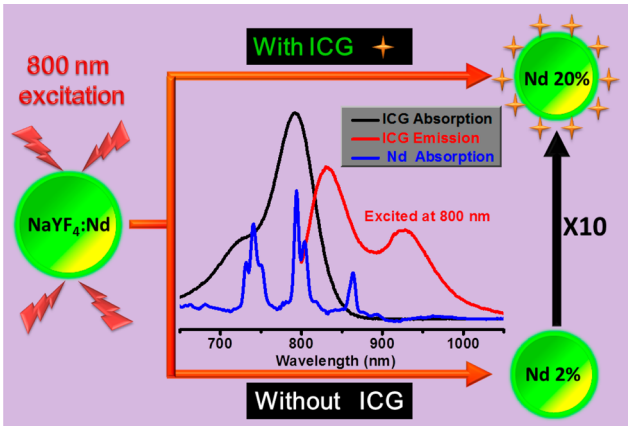

hexagonal crystallographic phase (JCPDS No. 16-0334), favorable for high upconversion efficiency.[1g,7] Their UCL spectra are shown in Figure 1b. The optimal doping concentration for Nd^{3+} turned out to be around 2 mol% (inset of Figure 1b), similar to the optimized amount of other activators, Er^{3+}, Tm^{3+}, and Ho^{3+}, reported in the literature on UCNPs.[8] The quenching of UCL beyond this critical concentration is ascribed to the well-known concentration quenching effect existing in a majority of lanthanide ions. From Figure 1c, highly visible UCL can be observed from the $NaYF_4$:Nd UCNPs under 800 nm laser excitation. Interestingly, the emission color changed from green to orange with the elevated concentration of Nd^{3+}, in accordance with the spectral change in Figure 2b. This is presumably due to the cross relaxation process [$^4F_{3/2} \rightarrow {}^4I_{9/2}$:$^4I_{15/2} \rightarrow {}^2G_{7/2}/{}^4G_{5/2}$] between two Nd^{3+} ions (Figure S3), resulting in the population increase of the yellow-emitting $^2G_{7/2}$ and $^4G_{5/2}$ states.[9] The proposed underlying upconversion mechanism is shown in Figure 1d. Upon 800 nm excitation, the Nd^{3+} ions in the ground state $^4I_{9/2}$ are first excited to the $^4F_{5/2}/{}^2H_{9/2}$ states.[8c] Some Nd^{3+} ions in these excited states rapidly relax to the $^4F_{3/2}$ state through a multi-phonon-assisted process. The Nd^{3+} ions at the $^4F_{3/2}$ state are then promoted to higher excited states $^2D_{5/2}/{}^2P_{1/2}$ by absorbing a second photon or by energy transfer from a Nd^{3+} ion at the $^4F_{5/2}/{}^2H_{9/2}$ state.[5b,9b,d,e] Subsequently, two-photon emissions centered at 413, 523, 588, 640, and 661 nm emerge, which are attributed to $^2D_{5/2}/{}^2P_{1/2} \rightarrow {}^4I_{9/2}$, $^4G_{7/2}/{}^2K_{13/2}/{}^4G_{9/2} \rightarrow {}^4I_{9/2}$, $^2G_{7/2}/G_{5/2} \rightarrow {}^4I_{9/2}$, $^2H_{11/2} \rightarrow {}^4I_{9/2}$, and $^4F_{9/2} \rightarrow {}^4I_{9/2}$ transitions, respectively. The dependence of the UCL intensities for distinct bands on the excitation power density was measured, and the results are shown in Figure S4. The slopes of 523 and 588 nm UCL bands are determined to be 1.78 and 1.79, validating that the dominant emission bands originate from a two-photon process.

We next explored the optical behavior of a set of $NaYF_4$:Nd UCNPs (with different Nd^{3+} content) sensitized by ICG dye of various concentrations. To ensure a close contact between the

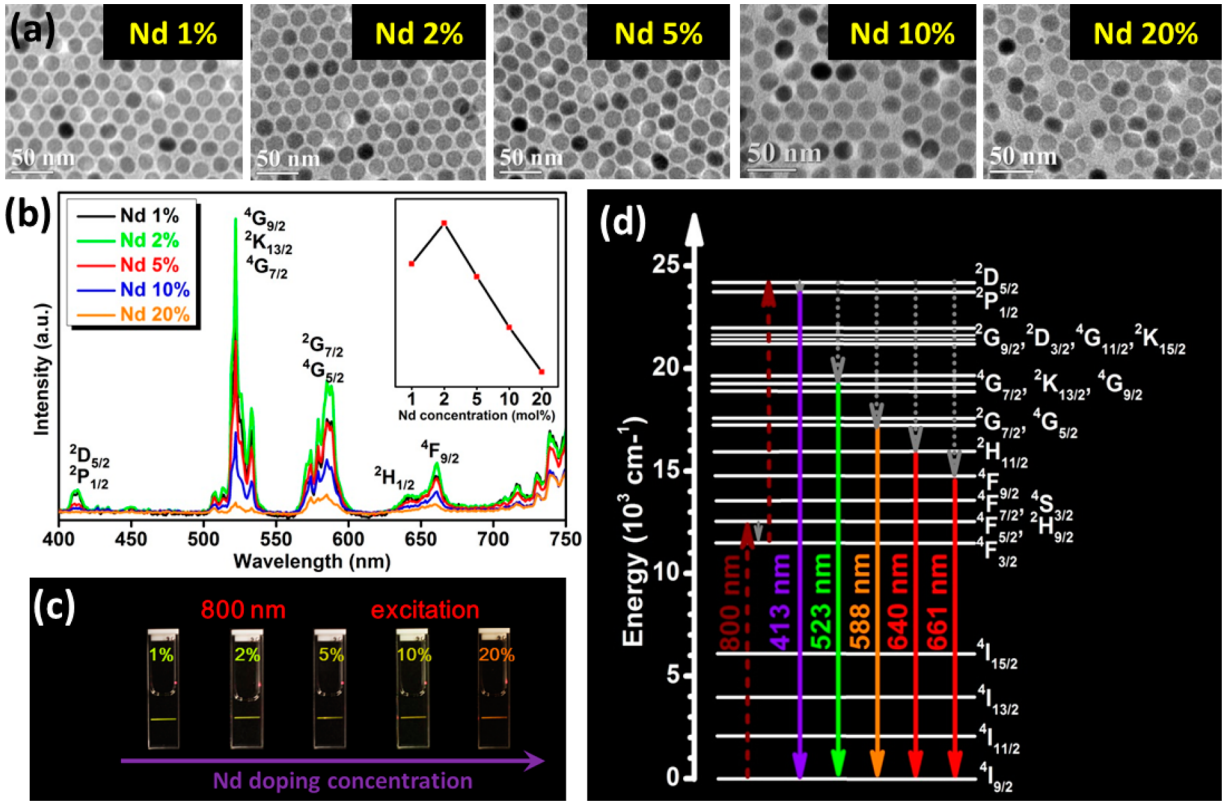

Figure 1. (a) TEM images of $NaYF_4$:Nd UCNPs with different Nd doping levels. (b) UCL spectra of the as-synthesized $NaYF_4$:Nd UCNPs under 800 nm excitation at a power of 1 W. The UCNPs were dispersed in hexane with a concentration of 13 mg/mL. Inset: Integrated intensity of entire emission (400 to 700 nm) as a function of Nd^{3+} doping concentration. (c) Corresponding luminescence photographs of $NaYF_4$:Nd UCNPs under 800 nm excitation at a power of 1 W (hexane dispersion, 1 wt%). (d) Proposed upconversion mechanism of Nd^{3+}-doped $NaYF_4$ UCNPs.

DOI: 10.1021/jacs.6b09474
J. Am. Chem. Soc. 2016, 138, 15130−15133

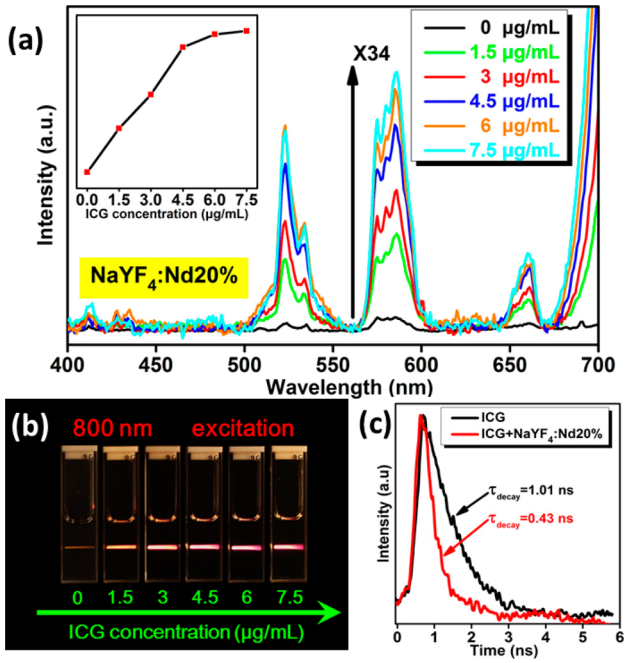

Figure 2. (a) UCL spectra of $NaYF_4$:Nd20% with different ICG concentrations under 800 nm excitation. Inset: Integrated intensity of entire emissions (400 to 700 nm) as a function of the ICG concentration. Note: The $NOBF_4$ coated $NaYF_4$:Nd20% UCNPs were dispersed in DMF at a concentration of 4.25 mg/mL. (b) Corresponding UCL photographs of $NaYF_4$:Nd20% UCNPs with different ICG concentrations. (c) Fluorescence lifetime curves of ICG with and without $NaYF_4$:Nd20% UCNPs.

UCNPs and ICG, the original oleic acid ligand capped on the as-synthesized nanoparticles was replaced by a short, ionic $NOBF_4$ ligand. Then the $NOBF_4$-coated UCNPs were dispersed in DMF for the following ICG sensitization experiment.[6a] Since 523 and 588 nm emissions are two dominant emissions in $NaYF_4$:Nd UCNPs (Figure 1b), our following investigations are mainly focused on these two emissions and all the emission intensity refers to integrated intensity. According to Figures 2a and S5−S10, the UCL intensities of all $NaYF_4$:Nd UCNPs were significantly improved with an increase amount of the ICG dye in solution, reaching a maximum at an ICG concentration of 6 μg/mL. Take the $NaYF_4$:Nd20% as an example (Figure 2a), the UCL intensity increases about 34 times at the optimal ICG concentration, when compared with that of the $NaYF_4$:Nd20% UCNPs alone. Figure 2b presents a clear UCL photograph of the increased brightness, providing the direct evidence of ICG sensitization under 800 nm excitation. We also measured the fluorescence decay curves of the ICG emission with and without the presence of $NaYF_4$:Nd20% UCNPs. As anticipated, the decay lifetime of the ICG dye was shortened from 1.01 to 0.43 ns due to the Förster-type non-radiative energy transfer from ICG to the surface Nd^{3+} ions. According to the equation $ET = 1 - \tau_{DA}/\tau_D$, where ET is the energy transfer efficiency and τ_{DA} and τ_D are the effective lifetimes of the energy donor in the absence and the presence of an energy acceptor,[6a] the efficiency for energy transfer from the ICG dye to the surface Nd^{3+} ions was estimated to be ~57%.

We then investigated the integrated UCL intensities of two dominant emissions at 523 and 588 nm from the $NaYF_4$:Nd UCNPs with and without ICG sensitization, as a function of Nd^{3+} concentration, summarizing the data from Figures 2a and S5−S10. As can be seen from Figure 3a, the sensitization effect

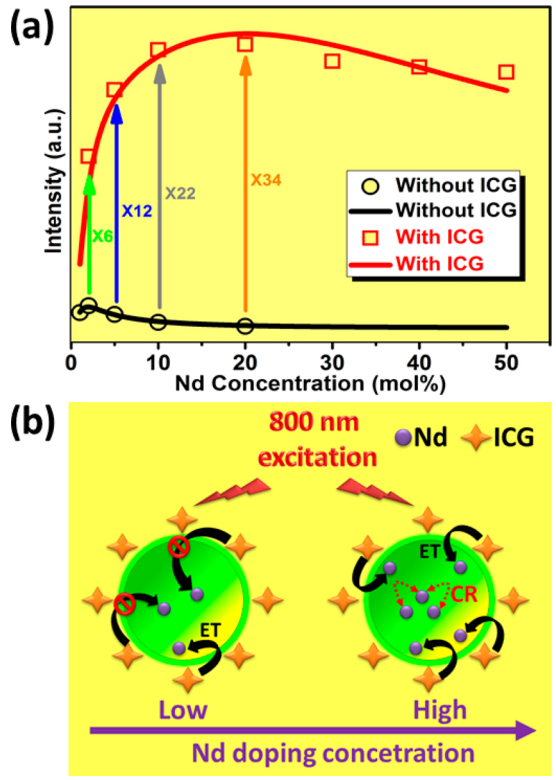

Figure 3. (a) Experimental results (black circle and red square) and theoretical modeling (black and red curves) of integrated UCL intensities of a set of $NaYF_4$:Nd UCNPs with (6.0 μg/mL) and without ICG sensitization. (b) Schematic illustration of the energy transfer mechanism from ICG to $NaYF_4$:Nd UCNPs, considering both low and high Nd^{3+} doping levels with ICG sensitization.

of ICG becomes more obvious at a higher Nd^{3+} doping level. About 6-, 12-, 22- and 34-fold UCL intensity increases were observed for 2, 5, 10, and 20 mol% Nd^{3+}-doped $NaYF_4$ UCNPs at the presence of 6.0 μg/mL ICG. This is reasonable, because when Nd^{3+} doping level is low, the amount of surface Nd^{3+} ions (the ions on or close to the UCNPs' surface) is low, producing a limited ICG sensitization effect. As the Nd^{3+} concentration increases, the amount of surface Nd^{3+} ions increases accordingly, introducing more channels to perform the ICG sensitization for every single $NaYF_4$:Nd UCNP. In Figure 3a, it should be noted that the optimal concentration for Nd^{3+} without the presence of ICG is 2 mol%, while it shifts to 20 mol% with the existence of ICG. This means that the luminescence concentration quenching effect, which occurs at a high doping level of the lanthanide ions owing to self-quenching (mostly, cross-relaxation-induced quenching process), was alleviated through the ICG dye sensitization. Along with the increment of Nd^{3+} concentration, the cross-relaxation process induced self-quenching becomes more pronounced to diminish UCL more, while on the other hand high Nd^{3+} doping concentration favors ICG sensitization, which enhances UCL intensity. Figure 3b briefly depicts the aforementioned competing processes that results in alleviation of luminescence concentration quenching effect. We envisioned that the coupling of enhanced NIR light harvesting due to the ICG dye having a ~30 000 times larger absorption section than Nd^{3+}

DOI: 10.1021/jacs.6b09474
J. Am. Chem. Soc. 2016, 138, 15130−15133

ions, the efficacious Förster-type energy transfer from the ICG dye to the surface Nd^{3+} ions (~57% efficiency), and subsequent efficient energy migration among the Nd^{3+} ions are able to activate the Nd^{3+} ions that can compete with the concentration-induced luminescence quenching rate. We developed a simple phenomenological model to interpret the kinetics of the sensitization behavior of ICG with the variation of Nd^{3+} doping concentration. In short, in estimating the emission intensity of the sensitized UCNPs, we assumed that sensitization could be accounted for the modified cross section of the one-photon excitation of Nd^{3+} ions, followed by either excited state absorption or energy transfer upconversion. The dimensionless prefactor that quantifies this modification depends on the number of ICG molecules anchored on the surface of UCNPs, the absorption cross section of ICG, and the rate of resonance energy transfer from ICG to the adjacent Nd^{3+} ions. The competing process—a combination of concentration dependent self-quenching and cross relaxation—was assumed to be a short-range bi-exponential interaction. The results of our modeling are in good agreement with the experimental observations (Figure 3a). The details of theoretical modeling can be found in the Supporting Information.

In conclusion, we described a simple strategy to alleviate the luminescence concentration quenching that is ubiquitous in lanthanide-based luminescent materials. The optimal doping concentration of Nd^{3+} in colloidal $NaYF_4$:Nd UCNPs was shifted from 2 to 20 mol% through sensitization by anchoring an ICG dye on the nanocrystal surface, along with ~10 times upconverting brightness increase. The dye sensitization effect (with enhanced light harvesting) as well as efficient energy migration among the Nd^{3+} ions leads to the optimal concentration shift and brightness increase by competing with the self-quenching effect. Our results open opportunities to realize a higher UCL intensity at higher activator doping concentration, improving the performance of UCNPs that are actively engaged in a number of photonic applications.

■ ASSOCIATED CONTENT

Supporting Information

The Supporting Information is available free of charge on the ACS Publications website at DOI: 10.1021/jacs.6b09474.

Additional experimental details and characterization, including Figures S1−S10, and equations for calculations and modeling (PDF)

■ AUTHOR INFORMATION

Corresponding Author

*pnprasad@buffalo.edu

ORCID

Wei Wei: 0000-0002-9131-6275

Notes

The authors declare no competing financial interest.

■ ACKNOWLEDGMENTS

This work was supported by a grant from the U.S. Air Force Office of Scientific Research (No. FA9550-15-1-0358).

■ REFERENCES

(1) (a) Wang, F.; Liu, X. *Chem. Soc. Rev.* **2009**, *38*, 976. (b) Wang, Y.-F.; Liu, G.-Y.; Sun, L.-D.; Xiao, J.-W.; Zhou, J.-C.; Yan, C.-H. *ACS Nano* **2013**, *7*, 7200. (c) Chen, G.; Qiu, H.; Prasad, P. N.; Chen, X. *Chem. Rev.* **2014**, *114*, 5161. (d) Huang, X.; Han, S.; Huang, W.; Liu, X. *Chem. Soc. Rev.* **2013**, *42*, 173. (e) Zhang, C.; Yang, L.; Zhao, J.; Liu, B.; Han, M.-Y.; Zhang, Z. *Angew. Chem., Int. Ed.* **2015**, *54*, 11531. (f) Wu, X.; Zhang, Y.; Takle, K.; Bilsel, O.; Li, Z.; Lee, H.; Zhang, Z.; Li, D.; Fan, W.; Duan, C.; Chan, E. M.; Lois, C.; Xiang, Y.; Han, G. *ACS Nano* **2016**, *10*, 1060. (g) Zhang, Y.; Wei, W.; Das, G. K.; Yang Tan, T. T. *J. Photochem. Photobiol., C* **2014**, *20*, 71.

(2) (a) Liu, X.; Kong, X.; Zhang, Y.; Tu, L.; Wang, Y.; Zeng, Q.; Li, C.; Shi, Z.; Zhang, H. *Chem. Commun.* **2011**, *47*, 11957. (b) Dong, H.; Sun, L.-D.; Yan, C.-H. *Chem. Soc. Rev.* **2015**, *44*, 1608.

(3) Zhao, J.; Jin, D.; Schartner, E. P.; Lu, Y.; Liu, Y.; Zvyagin, A. V.; Zhang, L.; Dawes, J. M.; Xi, P.; Piper, J. A.; Goldys, E. M.; Monro, T. M. *Nat. Nanotechnol.* **2013**, *8*, 729.

(4) (a) De Boni, L.; Mendonça, C. R. *J. Phys. Org. Chem.* **2011**, *24*, 630. (b) Hirsch, L. R.; Stafford, R. J.; Bankson, J. A.; Sershen, S. R.; Rivera, B.; Price, R. E.; Hazle, J. D.; Halas, N. J.; West, J. L. *Proc. Natl. Acad. Sci. U. S. A.* **2003**, *100*, 13549.

(5) (a) Merkle, L. D.; Dubinskii, M.; Schepler, K. L.; Hegde, S. M. *Opt. Express* **2006**, *14*, 3893. (b) Xu, L.; Zhao, H.; Xu, C.; Zhang, S.; Zhang, J. *J. Appl. Phys.* **2014**, *116*, 063104. (c) Jaque, D.; Martinez Maestro, L.; del Rosal, B.; Haro-Gonzalez, P.; Benayas, A.; Plaza, J. L.; Martin Rodriguez, E.; Garcia Sole, J. *Nanoscale* **2014**, *6*, 9494.

(6) (a) Chen, G.; Damasco, J.; Qiu, H.; Shao, W.; Ohulchanskyy, T. Y.; Valiev, R. R.; Wu, X.; Han, G.; Wang, Y.; Yang, C.; Ågren, H.; Prasad, P. N. *Nano Lett.* **2015**, *15* (11), 7400−7407. (b) Chen, G.; Ohulchanskyy, T. Y.; Liu, S.; Law, W.-C.; Wu, F.; Swihart, M. T.; Ågren, H.; Prasad, P. N. *ACS Nano* **2012**, *6*, 2969.

(7) Wang, F.; Han, Y.; Lim, C. S.; Lu, Y.; Wang, J.; Xu, J.; Chen, H.; Zhang, C.; Hong, M.; Liu, X. *Nature* **2010**, *463*, 1061.

(8) (a) Wang, F.; Liu, X. *J. Am. Chem. Soc.* **2008**, *130*, 5642. (b) Teng, X.; Zhu, Y.; Wei, W.; Wang, S.; Huang, J.; Naccache, R.; Hu, W.; Tok, A. I. Y.; Han, Y.; Zhang, Q.; Fan, Q.; Huang, W.; Capobianco, J. A.; Huang, L. *J. Am. Chem. Soc.* **2012**, *134*, 8340. (c) Xie, X.; Gao, N.; Deng, R.; Sun, Q.; Xu, Q.-H.; Liu, X. *J. Am. Chem. Soc.* **2013**, *135*, 12608.

(9) (a) Zuegel, J. D.; Seka, W. *Appl. Opt.* **1999**, *38*, 2714. (b) Méndez-Ramos, J.; Abril, M.; Martín, I. R.; Rodríguez-Mendoza, U. R.; Lavín, V.; Rodríguez, V. D.; Núñez, P.; Lozano-Gorrín, A. D. *J. Appl. Phys.* **2006**, *99*, 113510. (c) Iparraguirre, I.; Balda, R.; Voda, M.; Al-Saleh, M.; Fernandez, J. *J. Opt. Soc. Am. B* **2002**, *19*, 2911. (d) Wang, X.; Song, J.; Sun, H.; Xu, Z.; Qiu, J. *Opt. Express* **2007**, *15*, 1384. (e) Li, M.; Hao, Z. H.; Peng, X. N.; Li, J. B.; Yu, X. F.; Wang, Q. Q. *Opt. Express* **2010**, *18*, 3364.

DOI: 10.1021/jacs.6b09474
J. Am. Chem. Soc. 2016, 138, 15130−15133